Desalination and Water Treatment
www.deswater.com
doi: 10.5004/dwt.2017.21482

94 (2017) 100–108
October

Enhanced dewaterability of sewage sludge by Fe^{2+}-activated persulfate oxidation under mild temperature

Qiao Xiong[a,b], Min Zhou[a], Mengjia Liu[a], Yi Han[a], Haobo Hou[a,b,*]

[a]*School of Resource and Environment Science, Wuhan University, Wuhan 430072, China, email: whuxiongqiao@163.com (Q. Xiong), zhoumin@whu.edu.cn (M. Zhou), whuliumengjia@163.com (M. Liu), yihan@whu.edu.cn (Y. Han), Tel. +86-187-71025991, email: hhb-bhh@163.com (H. Hou)*
[b]*Hubei Environmental Remediation Material Engineering Technology Research Center, Wuhan 430072, China*

Received 12 April 2017; Accepted 21 September 2017

ABSTRACT

We investigated the improvement in dewaterability of sewage sludge by two-valent iron activated persulfate oxidation process under mild temperature. Sludge dewaterability was found to be improved in this system. Capillary suction time (CST) and setting property were used to characterize sludge dewatering. Zeta potential, Fourier-transformed infrared (FT-IR) spectroscopy, scanning electronic microscopy (SEM), three-dimensional excitation-emission matrix (EEM) fluorescence spectroscopy, thermogravimetry (TG) and differential scanning calorimetry (DSC) analyses were used to explore influencing mechanisms. The optimal conditions to achieve the highest CST reduction efficiency (95.3% reduction within 3 min) in room temperature were found to be 62.9 mg persulfate ($S_2O_8^{2-}$) g^{-1} dry solid (DS), 19.6 mg Fe^{2+} g^{-1} DS, and pH 5. SEM images revealed the rupture of sludge flocs; EEM, TG-DSC, and FT-IR analyses indicated that the degradation of protein-like and polysaccharide-like substances in extracellular polymeric substances (EPS), which contributed to the release of EPS-bound water and interstitial water trapped between flocs, as well as subsequent enhanced dewaterability.

Keywords: Sewage sludge; Dewaterability; Two-valent iron; Persulfate oxidation

1. Introduction

The treatment and disposal of Sewage sludge (SS), which is a by-product of municipal wastewater treatment, is causing great concern among the general public and government regulatory agencies [1]. Improper use and disposal of SS causes severe environmental impacts and health hazard to the public because it contains abundant harmful substances such as pathogens, heavy metals and some organic contaminants [2]. In addition, high moisture content is a common characteristic of different types of sludge, dewatering is an important step for all proposed sludge management options for it reduces the volume of sludge and consequently decreases the costs of handing, transport and final disposal [3–5]. According to previous researches, the extracellular polymeric substances (EPS) is a major component in sludge floc matrixes and recognized as the key to the dewaterability of sludge [6,7]. Therefore, efforts have been put into how to degrade EPS, in which bound water retained.

Persulfate advanced oxidation technology, which used to degrade organic compounds and wastewater treatment, is a new but increasingly used technology based on the sulfate radicals ($SO_4\cdot^-$). Persulfate (PS) or peroxymonosulfate (PMS) can generate $SO_4\cdot^-$ radicals activated by ultraviolet light [8,9], heat [10], transit metals (Co^{2+}, Fe^{2+}, Ag^+) [11], or alkaline [12,13]. Fe^{2+} has been commonly used as the activator to generate $SO_4\cdot^-$ in practical application because of the advantages of cost effectiveness, high activity and the environmentally friendly nature [13]. $SO_4\cdot^-$ radical (E_0 = 2.65–3.10 V) regarded as an alternative to HO· radical (E_0 = 2.70–2.80 V) because of its high redox potential [14].

$Fe^{2+}/S_2O_8^{2-}$ oxidation has been applied to treat a variety of contaminants. For example, Shi et al. used

*Corresponding author.

Fe^{2+}-sodium persulfate as a conditioner for dewatering of waste activated sludge and the results indicate that Fe^{2+}-sodium persulfate conditioning resulted in the increase of dewatering efficiency of sludge [15]. Zhen et al. [16] investigated the potential benefits of Fe(II)-activated persulfate ($S_2O_8^{2-}$) oxidation under mild temperature in enhancing the dewaterability of waste activated sludge and explored influencing mechanisms of dewatering process. Khandarkhaeva et al. [17] studied the oxidation of s-triazines by a solar-enhanced Fenton-like process involving persulfate and ferrous iron which showed great degradation efficiency. Ismail et al. [18] evaluated of different persulfate activation methods (UV, solar light, electron, Fe(II)) on the degradation of sulfaclozine along with the effect of persulfate concentrations. Therefore, persulfate advanced oxidation technology could be an effective way for sludge dewatering.

In this study, $Fe^{2+}/S_2O_8^{2-}$ oxidation pretreatment for SS in mild temperature were elucidated. Capillary suction time (CST) and setting property were characterized to evaluate the sludge dewaterability. Zeta potential was measured to explain the changes observed in sludge conditioning process. Scanning electronic microscopy (SEM), fourier-transformed infrared (FT-IR) spectroscopy, three-dimensional excitation-emission matrix (EEM) fluorescence spectroscopy, thermogravimetry (TG) and differential scanning calorimetry (DSC) were also performed to better understand the possible mechanisms of sludge dewatering. The effects of the different experimental conditions, $S_2O_8^{2-}$ dosage, Fe^{2+} dosage, pH and treat temperature on the dewatering capacity were conducted.

2. Materials and methods

2.1. Raw sludge

Raw sludge used in this study was a mixture of sludges from the primary and secondary sedimentation tanks of Sanjintan Wastewater Treatment Plant, Wuhan, China. Municipal wastewater of 315 m^3/d was treated in this plant. Raw sludge samples were collected in polypropylene containers and stored at 4°C in a refrigerator. Before experiment, the raw sludge was taken out of the refrigerator and put in environmental condition until the temperature raised to 20°C. The characteristics of raw sludge were tested according to the standard methods (US EPA1995). The main characteristics of the raw sludge are shown in Table 1, and its inorganic elemental compositions (Si, Al, Fe, K and Na, etc.) were analyzed by an X-ray fluorescence (XRF) analyzer (X-Lab 2000). The contents of major inorganic oxides in the raw sludge are shown in Table 2.

Table 1
The main characteristics of the raw sludge

Indicator	Value
Moisture(%)	87.2 ± 2.22
pH	8 ± 1.03
Organic content (%)	35.3 ± 0.89
CST (s)	145 ± 3.08

Table 2
Contents of major inorganic oxides in the raw sludge (%)

Sample	Raw sludge
SiO_2	32.26
Al_2O_3	10.27
Fe_2O_3	8.78
P_2O_5	5.04
CaO	3.17
SO_3	1.62
MgO	1.43
K_2O	1.21
TiO_2	0.62
Na_2O	0.38
MnO	0.20
Others	0.29
LOI	34.73

2.2. Materials

Sodium persulfate (SPS) ($Na_2S_2O_8$, purity > 99.9 wt.%), ferrous sulfate ($FeSO_4{\cdot}7H_2O$, purity > 99.0 wt.%), sodium chloride (NaCl), hydrochloric acid (HCl) and sodium hydroxide (NaOH) were analytical reagents (Sinopharm Chemical Reagent, China) and were used without further purification. The required amount of SPS and Fe^{2+} solutions were freshly prepared immediately prior to the experiments. Deionized water was used in the whole experiment.

2.3. Experimental procedures

Initially, 100 g raw sludge samples were carefully transferred to 500 mL beakers and stirred for 30 min to make sure the sludge particles evenly mixed with water. Before conditioned, the initial water content of sludge was diluted to 95% for equal treatment. And then conditioned in accordance with the following procedure: adding SPS → 3 min of rapid mixing at 500 rpm → adding $FeSO_4{\cdot}7H_2O$ solution (solid to liquid ratio = 1:10) → 5 min of rapid mixing at 500 rpm. At predetermined time intervals, a 5.0 mL sample was withdrawn and tested for its dewaterability at room temperature. The sludge samples after conditioned were centrifuged at 5000 rpm for 10 min to collect the supernatant and precipitates which were dried at 105°C for 24 h and used for mechanism investigation. The experimental set-up of the sludge conditioning system is shown in Fig. 1.

2.4. Analytical methods

CST (capillary suction time) and settling property were used to evaluate sludge dewatering performance in this study. The CST was measured by a 304M CST equipment (Triton, UK) at 25°C. Slurry is poured into the 10-mm-diameter tube resting on a piece of filter paper and the time was recorded automatically. The CST reduction efficiency (Y) was calculated as follows: , where CST_b (s) is

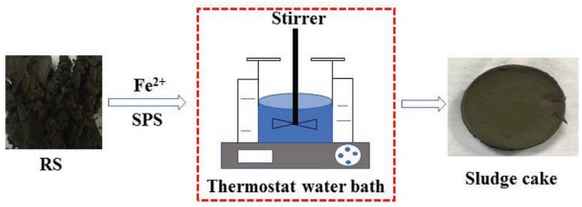

Fig. 1. Schematic diagram of experimental set-up.

the initial CST of raw sludge, and CST_f is the CST of sludge after conditioned by $S_2O_8^{2-}$ and Fe^{2+}. The settling property was determined by the following procedure: 100 mL raw and conditioned sludge were transferred to measuring cylinder, then recorded the interface position every 10 min in 90 min. The zeta potential was tested using a Malvern Zetasizer Nano ZS (Malvern Instruments Ltd, UK). The pH was tested by a pH meter (HM-30V, TOA, JAPAN). The morphology of the obtained samples was observed by SEM (JSM5610LV). The chemical bonds on the surface of the catalysts were detected by FT–IR spectroscopy (Nexus, Thermo Nicolet). All the EEM fluorescence spectra were measured using a luminescence spectrometry (FluoroMax-4, HORIBA Jobin Yvon Co., France). The EEM spectra were gathered with the scanning emission (Em) spectra from 250 to 550 nm at 5 nm increments by varying the excitation (Ex) wavelength from 250 to 400 nm at 5 nm increments. Excitation and emission slits were both maintained at 5 nm, and the scanning speed was set at 4800 nm/min for all the measurements. TG-DSC analysis was performed to determine the amount of total and bound water in sludge cake. A thermal analyzer (STA449c/3/G, NETZSCH, Germany) was employed to record thermographs of the sludge cake. Pure N_2 was used as the carrying gas. The amount of total water (W_t) is defined as the sludge weight loss when the temperature raised from 30°C to 150°C [19]. The bound water content was determined using a Q2000 differential scanning calorimetry (DSC) analyzer (TA, USA). DSC curve was obtained by fast cooling from room temperature to –20°C, followed by a reheating to 10°C at a rate of 2°C/min. The amount of free water (W_f) was calculated as follows: $W_f = Q/\Delta H$, where Q is the heat absorbed during melting process and ΔH is the melting enthalpy of free water (ΔH = 333.3 J/g). The bound water (W_b) was calculated as the difference between W_t and W_f [20].

3. Results and discussion

3.1 SEM analysis

The SEM images of the filter cake of raw and conditioned sludge were shown in Fig. 2. It can be seen from Fig. 2a and 2b that the surface of raw sludge flocs seems to be smooth and less porosity, Fig. 2c and 2d show that the massive sludge floc disintegrated to many smaller flocs, and forming many pores after treated by $Fe^{2+}/S_2O_8^{2-}$ oxidation at room temperature. Fig. 2e and 2f also indicate that the collapse of the flocs and a significant increase in porosity, which may be attributed to the degradation of EPS. Its degradation can make the bound water and interstitial water trapped between the flocs released into the free water, and therefore enhanced the dewaterability of sludge.

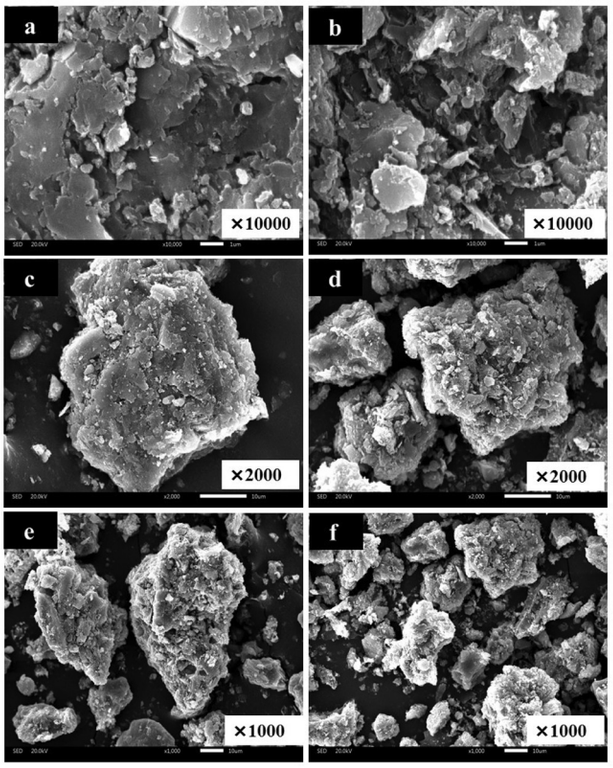

Fig. 2. SEM images of (a, c, e) raw sludge and (b, d, f) sludge after conditioned by $Fe^{2+}/S_2O_8^{2-}$ at room temperature.

3.2. FT-IR analysis

The FT-IR spectra of raw sludge and conditioned sludge are illustrated in Fig. 3. The band at 3409 cm^{-1} is

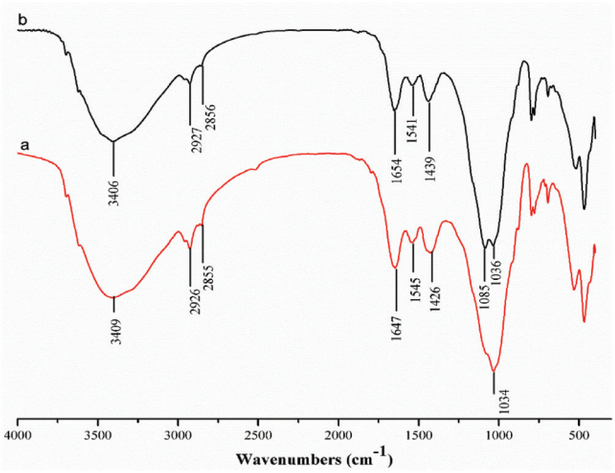

Fig. 3. FT-IR spectra of (a) raw sludge and (b) the sludge after conditioned by $Fe^{2+}/S_2O_8^{2-}$ at room temperature.

the O–H stretching vibration [21]. The bands at 2926 and 2855 cm^{-1} corresponded to the asymmetric and symmetric stretching vibrations of CH_2 of aliphatic structures and lipids, respectively [22,23]. The nature of functional groups present in the sludge flocs may predominantly originate from the EPS compositions [24]. The broad bands at 1647 and 1545 cm^{-1} are of protein origin (Amide I and Amide II, correspondingly), and shift to 1654 and 1541 cm^{-1} respectively following $Fe^{2+}/S_2O_8^{2-}$ oxidation, indicating the degradation and removal of protein-like substances in EPS [22]. The band at 1426 cm^{-1} corresponded to phenolic O–H and C–O stretching [25]. The band at 1034 cm^{-1} was due to the C–O–C and C–O vibration of polysaccharides, the intensity decreased following $Fe^{2+}/S_2O_8^{2-}$ oxidation, indicating the degradation and removal of polysaccharide-like substances in EPS. The bands at <1000 cm^{-1} were the "fingerprint" zone of phosphate or sulfur functional groups.

3.3. Fluorescence spectroscopy analysis

It is reported that EPS are regarded as one of the most important factors that influence the dewatering characteristics of sludge [26]. Typical EEM fluorescence spectroscopy of EPS and its corresponding fractions extracted from the raw and conditioned sludge are depicted in Fig. 4. It is evident from the results of Fig. 4 that persulfate oxidation results in more considerable changes in the fluorescent characteristics of soluble EPS compared to bound EPS. After conditioned,

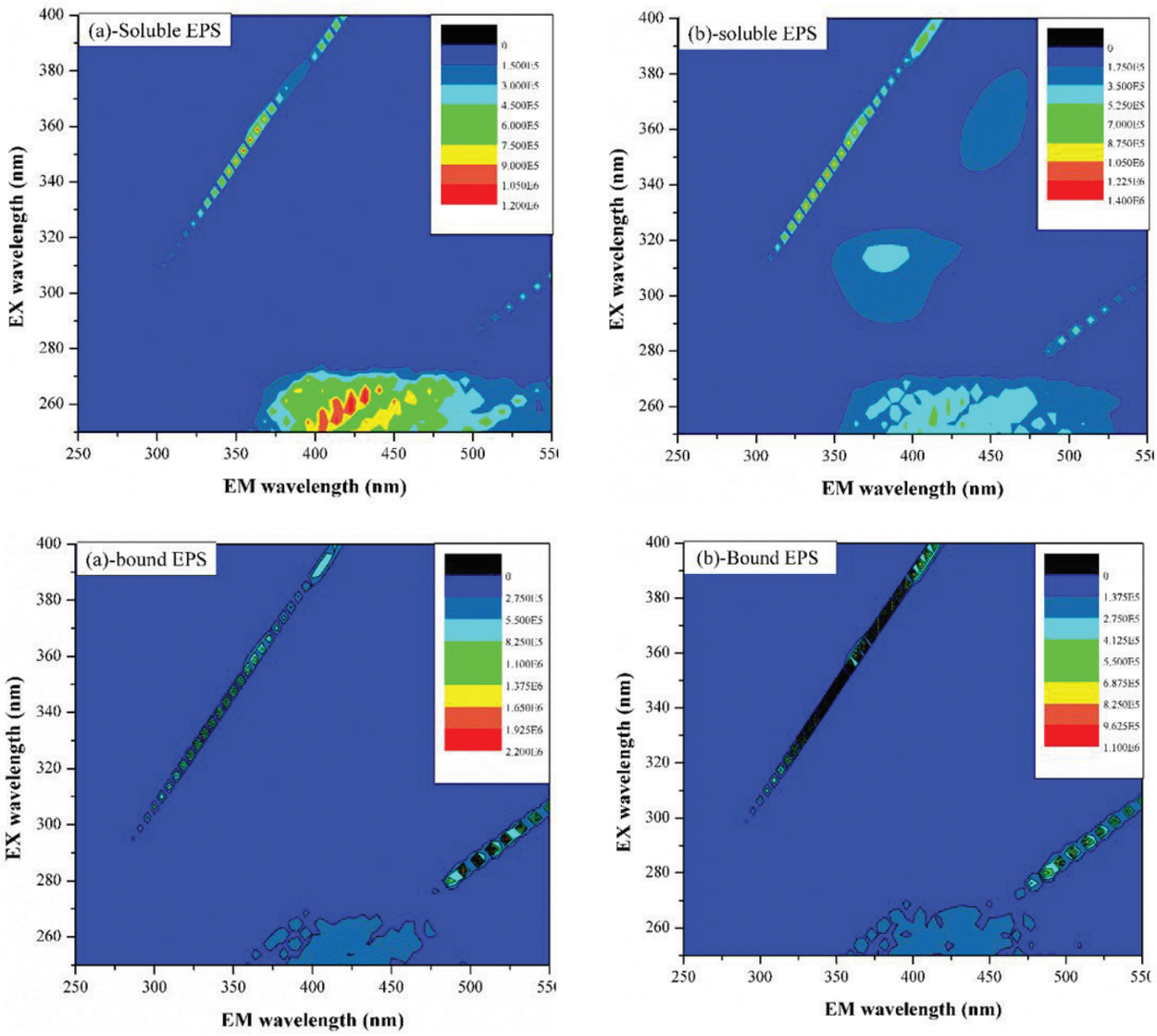

Fig. 4. EEM fluorescence spectra of the soluble and bound EPS fractions of (a) raw sludge and (b) the sludge after conditioned by $Fe^{2+}/S_2O_8^{2-}$ at room temperature.

only two peaks with much lower fluorescence intensity were identified at the excitation/emission (Ex/Em) of 305–315/375–400 and 250–265/400–450 in soluble EPS in comparison with four peaks located at the Ex/Em of 250–260/400–420, 250–260/425–450, 250–260/450–470 and 250–260/470–500 in the raw sludge, suggesting that the partial soluble EPS were degraded oxidatively by the reactive free radicals from the decomposition of persulfate. In contrast, fluorescence EEM of bound EPS were not greatly affected, in which fluorescence peak was always presented at the Ex/Em of 250–260/400–450. It has reported that the sludge dewaterability was improved by the decreased amount of soluble EPS [27,28]. And because of the difference of methods of EPS extraction and sludge types as well as sludge concentrations, there are slight discrepancy in the roles of EPS on sludge dewaterability [29].

3.4. TG-DSC analysis

The degradation of EPS can result in the release of bound water in the sludge flocs. The total water can be calculated from the TG curves (Fig. 5a) and the free water can be obtained from the DSC thermograms (Fig. 5b) as the method mentioned above. The total water in raw sludge and the conditioned sludge are 0.780 and 0.602 g/g, respectively. The free water is 0.635 and 0.551 g/g, respectively. The conditioned sludge can reduce bound water from 0.145 to 0.051 g/g. The results indicated that the bound water of sludge decreased after conditioned by $Fe^{2+}/S_2O_8^{2-}$, which showed that $Fe^{2+}/S_2O_8^{2-}$ is an effective way to enhance the sludge dewatering performance.

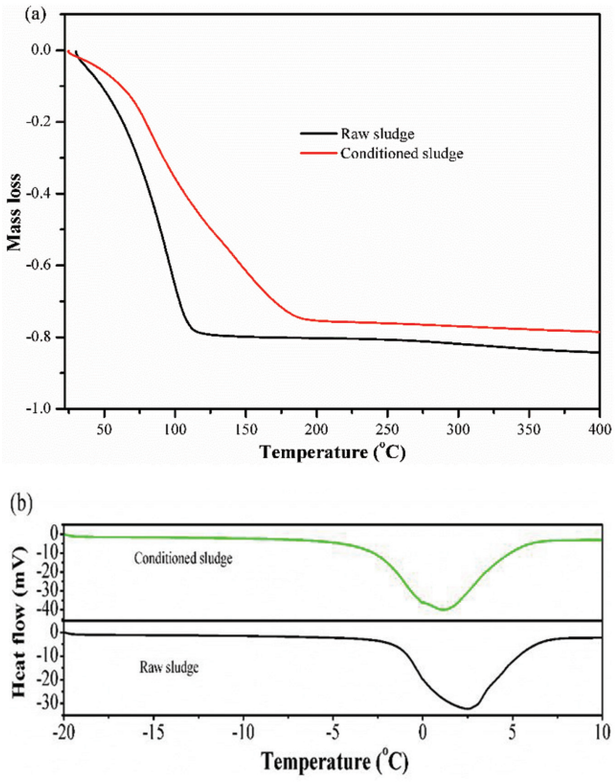

Fig. 5. (a) TG curve (b) DSC thermograms of raw sludge and sludge conditioned by $Fe^{2+}/S_2O_8^{2-}$.

3.5. Factors affecting effectiveness of sludge dewatering

To evaluate the effect of each component of the experimental procedure on sludge dewatering capacity, a series of single-factor experiments were conducted. Factors under evaluations included different experimental conditions, $S_2O_8^{2-}$ dosage, Fe^{2+} dosage, pH and treatment temperature.

3.5.1. Effect of different experimental conditions

A set of experiments with different formulations were conducted, including sludge conditioned by Fe^{2+}, sludge conditioned by $S_2O_8^{2-}$and sludge conditioned by $Fe^{2+}/S_2O_8^{2-}$. The dosage of Fe^{2+} and $S_2O_8^{2-}$ are 19.6 mg/g DS and 62.9 mg/g DS, respectively. Raw sludge was used as the control. The dewatering performance of different sludges is shown in Fig. 6. It can be seen from Fig. 6a the CST reduction efficiency of sludge conditioned by Fe^{2+} and $S_2O_8^{2-}$ alone were 40% and 21%, respectively. After conditioned by $Fe^{2+}/S_2O_8^{2-}$, the CST reduced 95.5%, which showed that the high dewatering performance should be obtained by the addition of Fe^{2+} and $S_2O_8^{2-}$ together.

It can be seen from Fig. 6b that the interface position of raw sludge was 96 mL after setting 90 min. Sludge conditioned by Fe^{2+}, $S_2O_8^{2-}$ and $Fe^{2+}/S_2O_8^{2-}$ reduced the interface position to 93.9, 88.2 and 70.6 mL, respectively, which illustrated that the $Fe^{2+}/S_2O_8^{2-}$ composite conditioner is feasible to improve the dewaterability of sludge.

3.5.2. Effect of the dosage of $S_2O_8^{2-}$

The effect of the dosage of $S_2O_8^{2-}$ in the range of 31.5–94.4 mg/g DS on the CST reduction efficiency and settling property over the $Fe^{2+}/S_2O_8^{2-}$ oxidation process at room temperature is shown in Fig. 7. And the dosage of Fe^{2+} is 15.6 mg/g DS. It can be seen from Fig. 7a and 7b that the highest CST reduction efficiency is 89.2% and sludge conditioned by $Fe^{2+}/S_2O_8^{2-}$ reduced the interface position to 79 mL after settling 90 min when $S_2O_8^{2-}$ dosage was 62.9 mg/g DS. So 62.9 mg/g DS $S_2O_8^{2-}$ was selected for the further studies.

3.5.3. Effect of the dosage of Fe^{2+}

The effect of the dosage of Fe^{2+} on the CST reduction efficiency over the $Fe^{2+}/S_2O_8^{2-}$ oxidation process at room temperature is illustrated in Fig. 8. From Fig. 8, the sludge dewatering capacity is the highest (93.1%) and the interface position reduced to 77 mL after settling 90 min when the Fe^{2+} dosage was 19.6 mg/g DS. So 19.6 mg/g DS $S_2O_8^{2-}$ was selected for the further studies.

Generally, the increase of the Fe^{2+} dosage could result in an increase of sludge dewaterability. However, the sludge dewaterability decreased with further increasing the amount of Fe^{2+}, which may be attributed to the reduce of $SO_4^{\cdot-}$ radicals and the reactions between persulfate and Fe^{2+} are shown in the following equations [30].

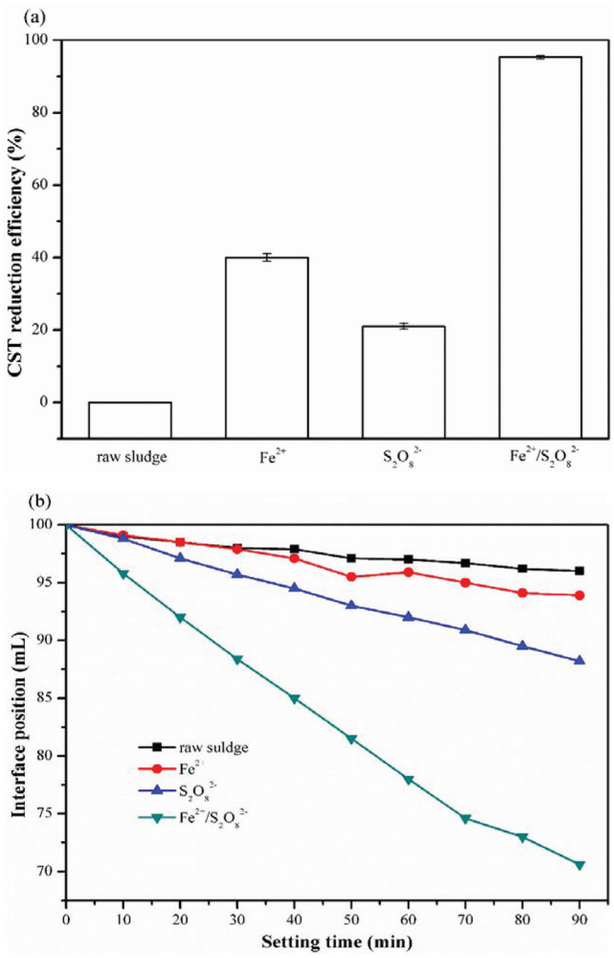

Fig. 6. Sludge dewatering performance: (a) CST reduction efficiency, (b) Settling property of the raw sludge and conditioned sludges under different formulations (Fe^{2+}-sludge conditioned by Fe^{2+}, $S_2O_8^{2-}$sludge conditioned by $S_2O_8^{2-}$, $Fe^{2+}/S_2O_8^{2-}$sludge conditioned by $Fe^{2+}/S_2O_8^{2-}$).

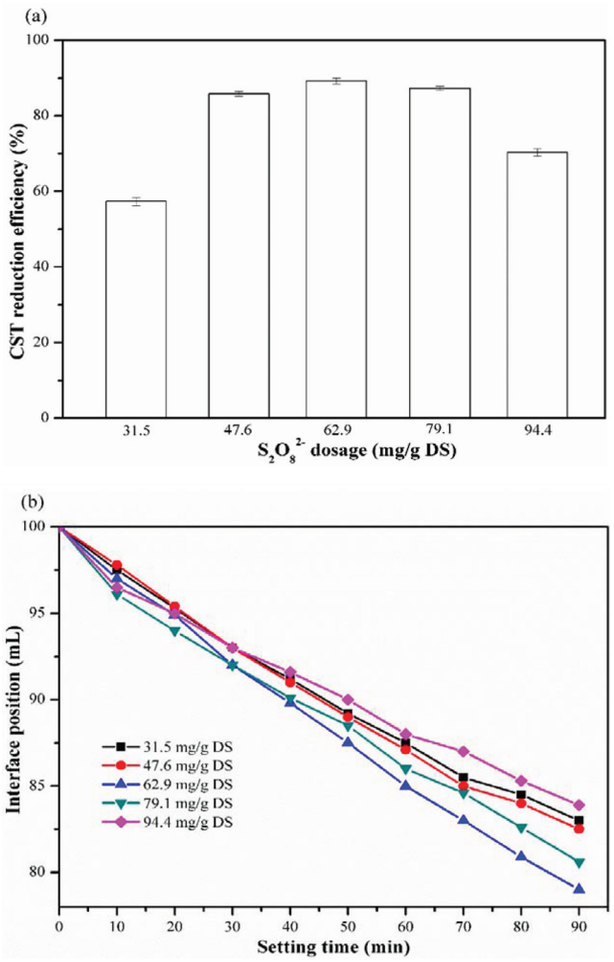

Fig. 7. Sludge dewatering performance: (a) CST reduction efficiency, (b) Settling property of the raw sludge and conditioned sludges with different $S_2O_8^{2-}$ dosage.

$$Fe^{2+} + 2S_2O_8^{2-} \rightarrow Fe^{3+} + SO_4\cdot^- + SO_4^{2-} \quad (1)$$

$$SO_4\cdot^- + Fe^{2+} \rightarrow Fe^{3+} + SO_4^{2-} \quad (2)$$

A high concentration of Fe^{2+} is required in the iron activated PS system since Fe^{2+} is hard to be regenerated after conversion to Fe^{3+} [31]. So, a proper Fe^{2+} dosage (19.6 mg/g DS) should be chosen. The excessive Fe^{2+} can act as a scavenger of $SO_4\cdot^-$ and iron sludge generated at the end of the treatment is not reusable requiring additional treatment and disposal [32].

3.5.4. Effect of the pH

It is reported that the large CST reduction should be obtained at near neutral pH [33]. So, in this study, pH from 5–10 was chosen. The CST reduction efficiency and settling property over the $Fe^{2+}/S_2O_8^{2-}$ oxidation process at different pH from 5 to 10 is shown in Fig. 9. As can be seen from Fig. 9(a), the sludge dewaterability were good with the CST reduction efficiency from 86.9% to 95.3%, which the highest efficiency was achieved at pH 5. The result shows that the CST reduction efficiency was more than 90% at pH 5–8, but comparatively lower at pH 9 and 10, this may be attributed to that $SO_4\cdot^-$ is stable in neutral and acidic solution, but can react as following equations in alkaline [34]. The results are consistent with previous research [32].

$$SO_4\cdot^- + H_2O \rightarrow HSO_4^- + HO\cdot \quad (3)$$

$$SO_4\cdot^- + OH^- \rightarrow SO_4^{2-} + HO\cdot \quad (4)$$

It can be seen from Fig. 9(b) that the settling property is consistent with the results of CST reduction efficiency.

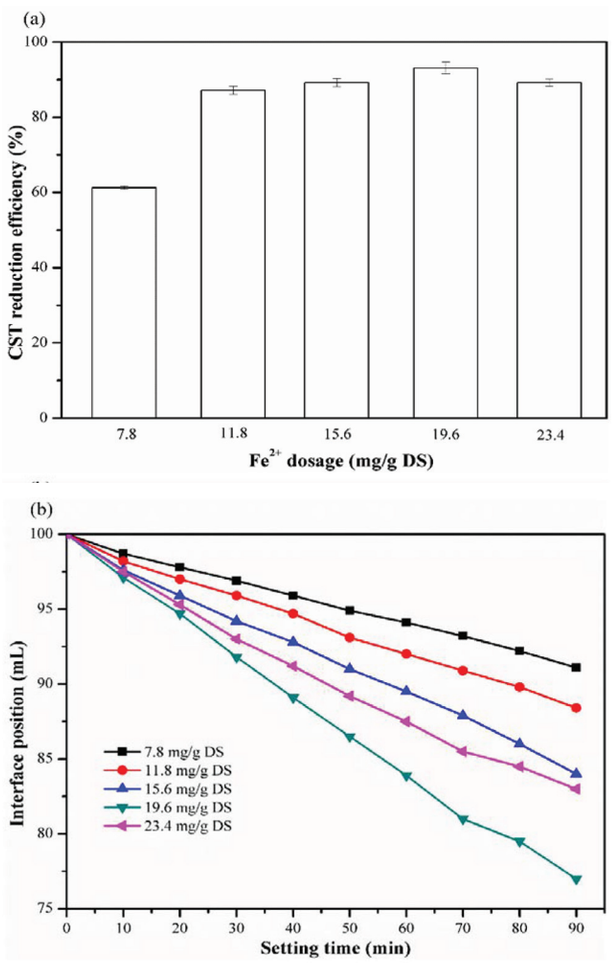

Fig. 8. Sludge dewatering performance: (a) CST reduction efficiency, (b) Settling property of the raw sludge and conditioned sludges with different Fe^{2+} dosage.

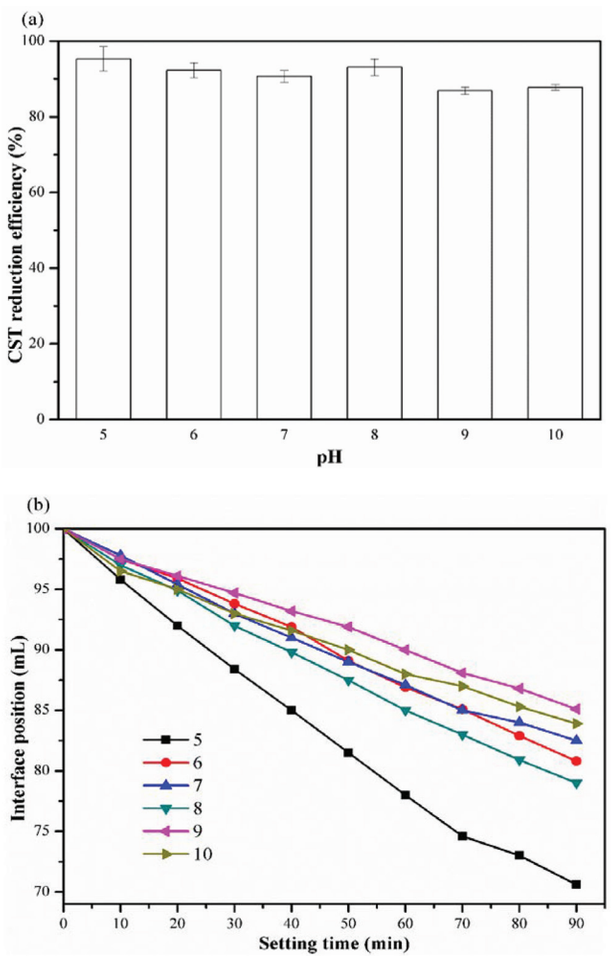

Fig. 9. Sludge dewatering performance: (a) CST reduction efficiency, (b) Settling property of the conditioned sludges at different pH.

The interface position of sludges is 70.6, 80.8, 82.5, 79, 85.1 and 83.9 mL at pH 5, 6, 7, 8, 9, 10, respectively. In result, $Fe^{2+}/S_2O_8^{2-}$ has a good oxidant effect in a range of pH from 5 to 10.

3.5.5. Effect of the treatment temperature

The CST reduction efficiency and settling property over the $Fe^{2+}/S_2O_8^{2-}$ oxidation process at different temperature is shown in Fig. 10. It can be found from Fig. 10(a) that the CST reduction efficiency were above 90% at all temperature, which show that the $Fe^{2+}/S_2O_8^{2-}$ oxidation can improve the sludge dewaterability in room temperature and mild temperature. And the interface position of sludges is 79, 80.6, 79, 78 and 80.9 mL when the condition temperature is room temperature, 40°C, 50°C, 60°C, 70°C, respectively. Therefore, $Fe^{2+}/S_2O_8^{2-}$ oxidation is a cost-effective and energy-efficient way for sludge dewatering. The results are in accordance with research by Zhen et al. [16].

3.6. The influence of zeta potential on the dewaterability

The zeta potential is a key factor in influencing sludge dewaterability. Fig. 11 presents the zeta potential evolution of sludge flocs treated by $Fe^{2+}/S_2O_8^{2-}$ oxidation under different temperatures. The surfaces of raw sludge were originally negatively charged with the zeta potential of –19.09 mV, and sharply increase to –5.726 mV after react with $Fe^{2+}/S_2O_8^{2-}$ at room temperature. The zeta potential showed no obvious shift with increasing temperature after $Fe^{2+}/S_2O_8^{2-}$ oxidation process. Combined with the CST reduction efficiency, the best dewaterability occurred at the highest zeta potential of –5.228 mV. This may due to that with the decreasing surface charge related to elevating zeta potential, the sludge can aggregate, settle down quickly and finally dewatered more easily [16].

4. Conclusions

$Fe^{2+}/S_2O_8^{2-}$ oxidation has been successfully demonstrated to be effective in enhancing the sludge dewatering capacity

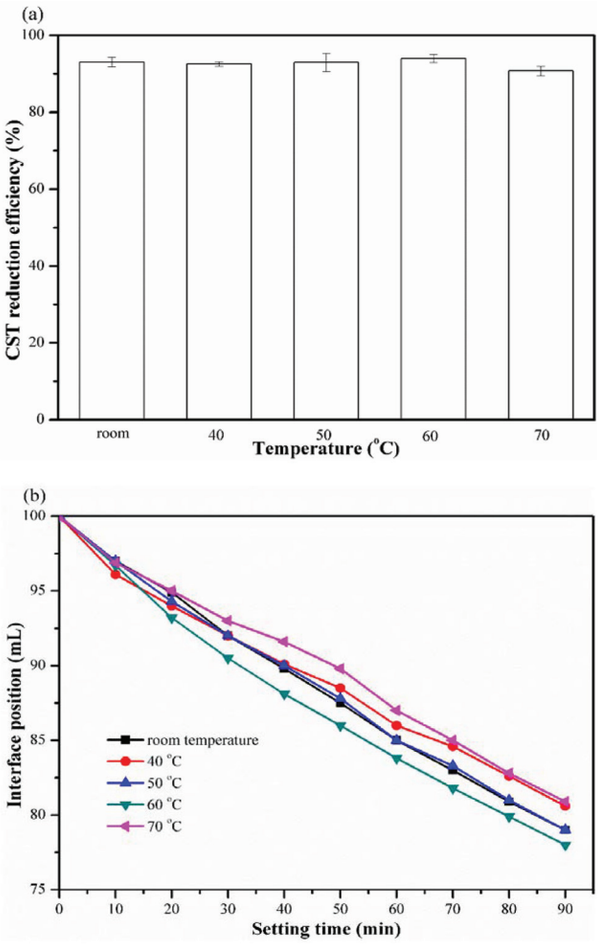

Fig. 10. Sludge dewatering performance: (a) CST reduction efficiency, (b) Settling property of the conditioned sludges with different treatment temperatures.

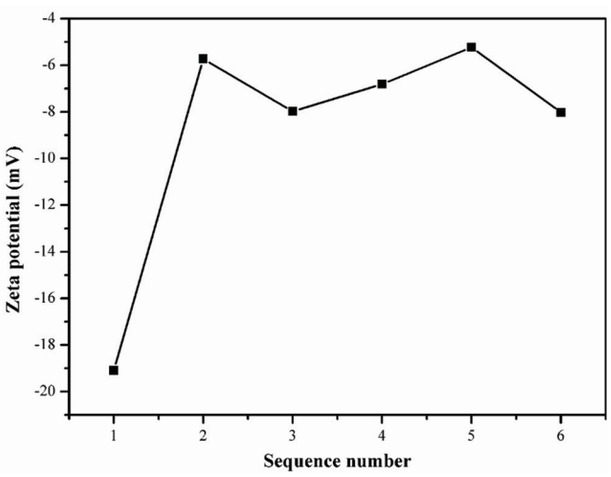

Fig. 11. Zeta potential evolution of sludge as a function of operational temperatures (1 – raw sludge; 2 – 40°C; 3 – 50°C; 4 – 60°C; 5 – 70°C; 6 – 80°C).

under mild temperature. Based on a series of single-factor experiments, a CST reduction efficiency of 95.3% was achieved in the optimal condition of this process. Decreasing negative potential and EPS content were mainly responsible for the observed changes in the dewaterability. EEM and FT-IR analysis showed that the degrading of protein-like substances and polysaccharide-like substances in EPS, SEM images revealed the rupture of sludge flocs, which contributed to the release of EPS-bound water and interstitial water trapped between flocs, and subsequent enhanced dewaterability. The results showed that the Fe^{2+}/$S_2O_8^{2-}$ oxidation could be a simple and efficient method for improving the dewaterability with a higher than 95% CST reduction.

Acknowledgments

This work was supported by the National Science & Technology Pillar Program, China (No. 2015BAB01B03).

References

[1] M. Seggiani, S. Vitolo, M. Puccini, A. Bellini, Cogasification of sewage sludge in an updraft gasifier, Fuel, 93 (2012) 486–491.
[2] A.L. Elled, L.E. Åmand, B. Leckner, B.Å. Andersson, Influence of phosphorus on Sulphur capture during co-firing of sewage sludge with wood or bark in a fluidized bed, Fuel, 85 (2006) 1671–1678.
[3] L. Bennamoun, P. Arlabosse, A. Léonard, Review on fundamental aspect of application of drying process to wastewater sludge, Renew. Sust. Energ. Rev., 28 (2013) 29–43.
[4] K. Mahmoud, J. Olivier, J. Vaxelaire. Advances in mechanical dewatering of wastewater sludge treatment. In: Wastewater Reuse and Management, Sharma, S.K., Sanghi, R., (Eds.), Springer, London, 2013, pp. 253–303.
[5] S.J. Skinner, L.J. Studer, D.R. Dixon, P. Hillis, C.A. Rees, R.C. Wall, R.G. Cavalida, S.P. Usher, A.D. Stickland, P.J. Scales, Quantification of wastewater sludge dewatering, Water Res., 82 (2015) 2–13.
[6] X.M. Liu, G.P. Sheng, H.W. Luo, S.J. Yuan, J. Xu, R.J. Zeng, J.G. Wu, H.Q. Yu, Contribution of extracellular polymeric substances (EPS) to the sludge aggregation, Environ. Sci. Technol., 44 (2010) 4355–4360.
[7] G.Y. Zhen, X.Q. Lu, Y.Y. Li, Y.C. Zhao, B.Y. Wang, Y. Song, X.L. Chai, D. J. Niu, X.Y. Cao, Novel insights into enhanced dewaterability of waste activated sludge by Fe(II)-activated persulfate oxidation, Bioresour. Technol., 119 (2012) 7–14.
[8] Y.Q. Gao, N.Y. Gao, Y. Deng, Y.Q. Yang, Y. Ma, Ultraviolet (UV) light-activated persulfate oxidation of sulfamethazine in water, Chem. Eng. J., 195–196 (2012) 248–253.
[9] T.K. Lau, W. Chu, N.J.D. Graham, The aqueous degradation of butylated hydroxyanisole by UV/S2O82: study of reaction mechanisms via dimerization and mineralization, Environ. Sci. Technol., 41 (2007) 613–619.
[10] R.H. Waldemer, P.G. Tratnyek, R.L. Johnson, J.T. Nurmi, Oxidation of chlorinated ethenes by heat-activated persulfate: kinetics and products, Environ. Sci. Technol., 41 (2007) 1010–1015.
[11] G.P. Anipsitakis, D.D. Dionysiou, Radical generation by the interaction of transition metals with common oxidants, Environ. Sci. Technol., 38 (2004) 3705–3712.
[12] Y. H. Guan, J. Ma, X. C. Li, J.Y. Fang, L.W. Chen, Influence of pH on the formation of sulfate and hydroxyl radicals in the UV/peroxymonosulfate system, Environ. Sci. Technol., 45 (2011) 9308–9314.
[13] A. Rastogi, S.R. Al-Abed, D.D. Dionysios, Effect of inorganic, synthetic and naturally occurring chelating agents on Fe(II) mediated advanced oxidation of chlorophenols, Water Res., 43 (2009) 684–694.

[14] T.C. An, H. Yang, G.Y. Li, W.H. Song, W.J. Cooper, X.P. Nie, Kinetics and mechanism of advanced oxidation processes (AOPs) in degradation of ciprofloxacin in water, Appl. Catal. B Environ., 94 (2010) 288–294.
[15] Y.F. Shi, J.K. Yang, W. Mao, Y.L. Li, X.Xu, H. Zhang, W.B. Yu, Y. Li, C.Z. Yang, Influence of Fe^{2+}-sodium persulfate on extracellular polymeric substances and dewaterability of sewage sludge, Desal. Water Treat., 53 (2015) 2655–2663.
[16] G.Y. Zhen, X.Q. Lu, B.Y. Wang, Y.C. Zhao, X.L. Chai, D.J. Liu, A.H. Zhao, Y.Y. Li, Y. Song, X.Y. Cao, Synergetic pretreatment of waste activated sludge by Fe(II)-activated persulfate oxidation under mild temperature for enhanced dewaterability, Bioresour. Technol. 124 (2012) 29–36.
[17] M. Khandarkhaeva, A. Batoeva, D. Aseev, M. Sizykh, O. Tsydenova, Oxidation of atrazine in aqueous media by solar-enhanced Fenton-like process involving persulfate and ferrous ion, Ecotoxicol. Environ. Saf., 137 (2017) 35–41.
[18] L. Ismail, C. Ferronato, L. Fine, F. Jaber, J.M. Chovelon, Elimination of sulfaclozine from water with SO4 radicals: Evaluation of different persulfate activation methods, Appl. Catal. B: Environ., 201 (2017) 573–581.
[19] L.F. Wang, D.Q. He, Z.H. Tong, W.W. Li, H.Q. Yu, Characterization of dewatering process of activated sludge assisted by cationic surfactants, Biochem. Eng. J., 9 (2014) 174–178.
[20] N. Katsiris, A. Kouzeli-Katsiri, Bound water content of biological sludges in relation to filtration and dewatering, Water Res., 21 (1987) 1319–1327.
[21] M. Kumar, S.S. Adham, W.R. Pearce, Investigation of seawater reverse osmosis fouling and its relationship to pretreatment type, Environ. Sci. Technol., 40 (2006) 2037–2044.
[22] O. Gulnaz, A. Kaya, S. Dincer, The reuse of dried activated sludge for adsorption of reactive dye, J. Hazard Mater. B, 134 (2006) 190–196.
[23] S. Amir, M. Hafidi, G. Merlina, J.C. Revel, Sequential extraction of heavy metals during composting of sewage sludge, Chemosphere, 59 (2005) 801–810.
[24] J. Laurent, M. Casellas, H. Carrère, C. Dagot, Effects of thermal hydrolysis on activated sludge solubilization surface properties and heavy metals biosorption, Chem. Eng. J., 166 (2011) 841–849.
[25] M. Grube, J.G. Lin, P.H. Lee, S. Kokorevicha, Evaluation of sewage sludge-based compost by FT-IR spectroscopy, Geoderma, 130 (2006) 324–333.
[26] Q. Yu, H. L. Lei, G. W. Yu, X. Feng, Z.X. Li, Z.C. Wu, Influence of microwave irradiation on sludge dewaterability, Chem. Eng. J., 155 (2009) 88–93.
[27] F.D. Sanin, P.A. Vesilind, Effect of centrifugation on the removal of extracellular polymers and physical properties of activated sludge, Water Sci. Technol., 30 (1994) 117–127.
[28] X.Y. Li, S.F. Yang, Influence of loosely bound extracellular polymericsubstances (EPS) on the flocculation, sedimentation and dewaterability of activated sludge, Water Res., 41 (2007) 1022–1030.
[29] T.L. Poxon, J.L. Darby, Extracellular polyanions in digested sludge:measurement and relationship to sludge dewaterability, Water Res., 31 (1997) 749–758.
[30] C.J. Liang, I.L. Lee, I.Y. Hsu, C.P. Liang, Y.L. Lin, Persulfate oxidation of trichloroethylene with and without iron activation in porous media, Chemosphere, 70 (2008) 426–435.
[31] I. Hussain, Y.Q. Zhang, S.B. Huang, X.Z. Du, Degradation of p-chloroaniline by persulfate activated with zero-valent iron, Chem. Eng. J., 203 (2012) 269–276.
[32] G.Y. Zhen, X.Q, X.Q. Lu, Y.C. Zhao, X.L. Chai, D.J. Niu, Enhanced dewaterability of sewage sludge in the presence of Fe(II)–activated persulfate oxidation, Bioresour. Technol., 116 (2012) 259–265.
[33] C.J. Liang, H.W. Su, Identification of sulfate and hydroxyl radicals in thermally activated persulfate, Ind. Eng. Chem. Res., 48 (2009) 5558–5562.
[34] X.Y. Wei, N.Y, Gao, C.J. Li, Y. Deng, S.Q. Zhou, L. Li, Zero-valent(ZVI)activation of persulfate (PS) for oxidation of bentazon in water, Chem. Eng. J., 285 (2016) 660–670.